



Review article

Recent advances and various detection strategies of deep eutectic solvents for zinc air batteries

Fentahun Adamu Getie^{a,b}, Delele Worku Ayele^{a,c,*}, Nigus Gabbiye Habtu^{a,d,**}, Temesgen Atnafu Yemata^d, Fantahun Aklog Yihun^e, Ababay Ketema Worku^a, Minbale Admas Teshager^c

^a Bahir Dar Energy Center, Bahir Dar Institute of Technology, Bahir Dar University, P.O. Box 26, Bahir Dar, Ethiopia

^b Department of Chemistry, College of Natural and Computational Science, Injibara University, P.O. Box 40, Injibara, Ethiopia

^c Department of Chemistry, College of Science, Bahir Dar University, P.O. Box 79, Bahir Dar, Ethiopia

^d Department of Chemical Engineering, Bahir Dar Institute of Technology, Bahir Dar University, P.O. Box 26, Bahir Dar, Ethiopia

^e Department of Industrial Chemistry, College of Science, Bahir Dar University, P.O. Box 79, Bahir Dar, Ethiopia

ARTICLE INFO

Keywords:

Deep eutectic solvents
Zinc-air batteries
Detection strategies
Stability

ABSTRACT

Sustainable technology in energy-related applications will be crucial in the coming decades. As a result, developing new materials for existing processes has presently arisen as a major research priority. Recently, Deep eutectic solvents (DESs) have been expected as low-cost task-specific solvents for zinc-air batteries (ZABs). Here in, initially the various preparation methods of DESs their detection strategies, and the fundamental characteristics of DESs are summarized. Then, the recent utilization of DESs on ZABs has been reviewed. After that, the chemical and physical characteristics of DESs including phase behavior, viscosity, density, ionic conductivity, refractive index, pH, surface tension and stability have been studied. Lastly, the challenges, limitations, and possible upcoming research fields of DESs for ZABs were discussed.

1. Introduction

Recent advancements in batteries have fascinated significant attention owing to their safe and environmentally friendly electrical energy storage capabilities [1]. Researchers are increasingly focused on developing a low-cost, safe, and clean energy storage systems, particularly metal-air batteries, as they provide numerous advantages [2]. These include high theoretical energy density, stable discharge voltages, long shelf life, environmental friendliness, high capacity, and low cost [1]. Various metal batteries for instance lead-acid batteries, nickel metal hydride (Ni-MH) batteries, and lithium-ion batteries (LIB) have already been commercialized. Nevertheless, they are still expensive [2,3]. Furthermore, there are concerns about raw material supply, safety issues, and hazards [4]. Hence, a battery system that satisfies both environmental and economic conditions is needed. Rechargeable zinc-air batteries (RZABs) have recently been explored due to their environmental friendliness, vast reserves, inherent safety, and attractiveness for large-scale energy storage systems [5,6]. To date, aqueous-based RZABs have dominated the market. However, problems with zinc (Zn) electrode passivation, hydrogen evolution, and dendrite development restrict their practical application [7]. To overcome these issues, RZABs

* Corresponding author. Bahir Dar Energy Center, Bahir Dar Institute of Technology, Bahir Dar University, P.O. Box 26, Bahir Dar, Ethiopia.

** Corresponding author. Bahir Dar Energy Center, Bahir Dar Institute of Technology, Bahir Dar University, P.O. Box 26, Bahir Dar, Ethiopia.

E-mail addresses: delelewww@gmail.com (D.W. Ayele), nigushabtu@gmail.com (N.G. Habtu).

<https://doi.org/10.1016/j.heliyon.2024.e40383>

Received 24 July 2024; Received in revised form 21 October 2024; Accepted 12 November 2024

Available online 15 November 2024

2405-8440/© 2024 Published by Elsevier Ltd.

This is an open access article under the CC BY-NC-ND license

(<http://creativecommons.org/licenses/by-nc-nd/4.0/>).

using non-aqueous electrolytes with high reversibility of Zn deposition and dissolution and voltage window with large operating have been used [8]. Moreover, to decrease the RZAB matters related to aqueous alkaline electrolytes, researchers have shown an interest in discovering substitute non-aqueous electrolyte systems [9]. Recently, deep eutectic solvents (DESs) (*i.e.*, non-aqueous electrolytes) as electrolytes for RZABs have been extensively investigated as they possess good air and moisture stability, low cost, low toxicity, simple preparation approach, nonvolatility, high electrochemical and thermal stability [10,11]. Numerous works have been studied on DESs for different industrial uses, including nanomaterials fabrication for energy storage applications [12], electrochemical energy storage and conversion technology in batteries electrolytes [13], supercapacitors technologies [14], fuel cells hierarchical carbon electrodes [15], solar energy applications [16], the preparation of energy storage functional materials [17], and in analytical extraction techniques [18]. For instance, Kheawhom et al. showed a stable biocompatible, and cost-effective $\text{ZnCl}_2/\text{ChCl}/\text{urea}$ DES electrolyte [2]. Their results indicated that no dendrites formed on the Zn metal surface, demonstrating highly reversible stripping and plating characteristics [19]. Furthermore, in redox flow batteries, eutectic electrolytes are also used as media for redox reactions to solubilize redox-active systems [20]. The eutectic electrolytes show numerous advantages, such as non-flammability, low volatility, and simpler synthesis than traditional organic solvents, and the redox-active systems undesirable solubility compromises the energy density of cell. These eutectic electrolytes offer several advantages, including non-flammability, low volatility, and simpler synthesis compared to conventional organic solvents. However, the redox-active systems undesirable solubility can compromise the cell energy density. Here in, we first review the mechanisms of electrolyte formation and their physicochemical properties [21]. Next, we highlighted the applications of eutectic electrolytes in ZABs and discussed the relations between their physicochemical characteristics, such as coordination environment, conductivity (ionic), concentration, viscosity, and the use of redox-active systems (materials). We then explained how eutectic electrolytes form specific electrode/electrolyte interfaces that enlarge the window of electrochemical while simultaneously inhibiting the metal dendrites growth in metal-based batteries. Finally, we concluded with a discussion on the findings and future prospects.

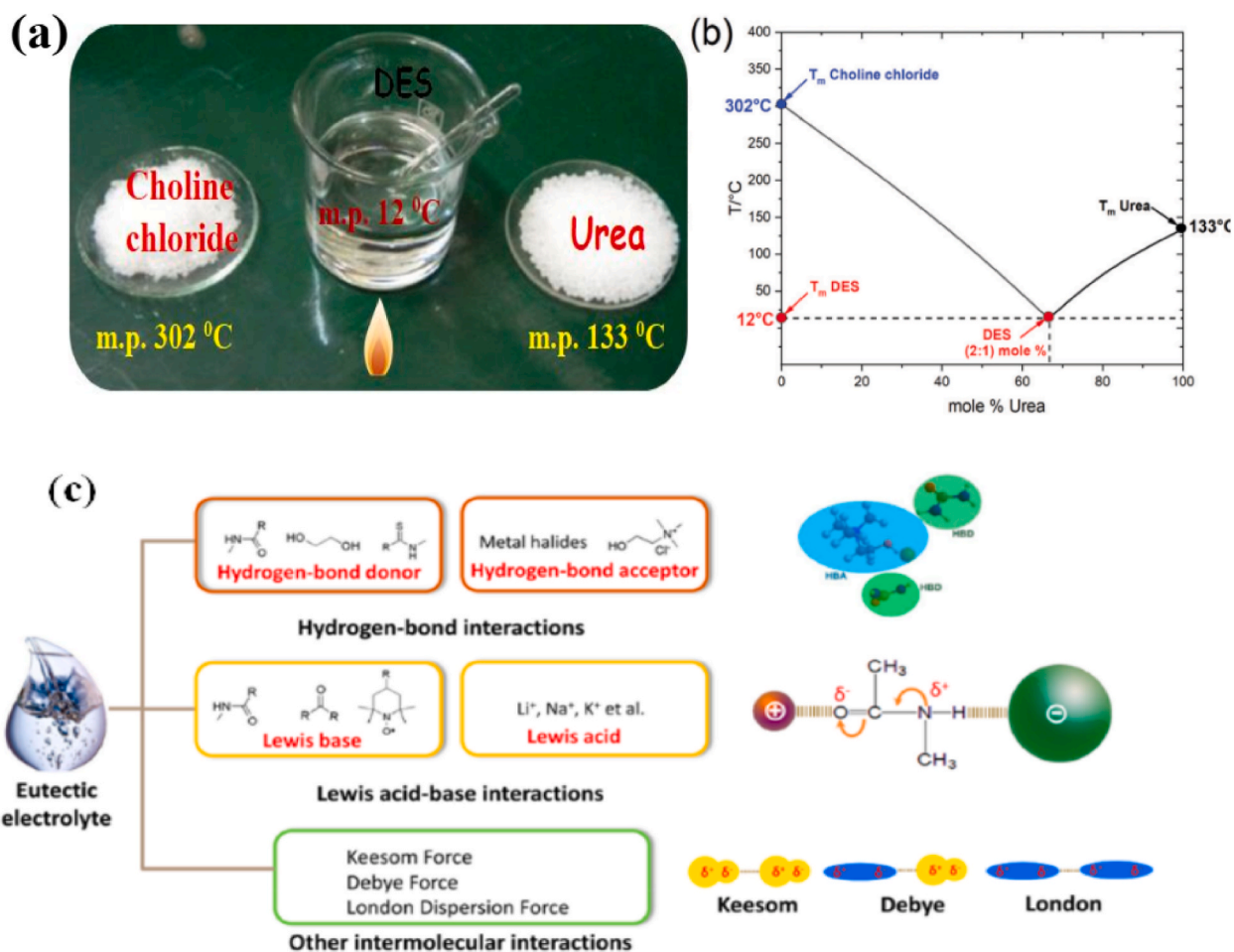


Fig. 1. (a) The choline chloride and urea (*i.e.* starting materials) are solids with high-melting points. Then when they mixed together created a liquid at room temperature. Reproduced with permission from Ref. [22] (b) Diagram representation of the comparison of equilibrium phase illustration of solid-liquid mixture of urea and choline chloride (Reline DES). Reproduced with permission from Ref. [23] (c) The mechanisms for the formation of eutectic electrolytes. Reproduced with permission from Ref. [10].

2. Overview of DESs

DESs, when combined with ionic liquids (ILs), are taken as green solvents [11]. They have got attention after a study by Abbott *et al.* that observed a deep melting point depression at the eutectic composition of hydrogen bond acceptors (HBAs) and hydrogen bond donors (HBDs) [22]. For instance, the mixture of urea/ChCl (2:1 mol ratio) attains a melting point of 12 °C which is much smaller than the melting point of the urea (133 °C) and ChCl (302 °C) making the liquid to be employed as room temperature solvent (Fig. 1a) [22]. Martins et al. also explained DES as the two or more pure compounds mixture in which the temperature of eutectic point is lower than an ideal liquid mixture and it shows a negative deviation from ideality [11]. The temperature depression is explained as the temperature difference (ΔT_2) between the ideal temperature and the deep eutectic point (Fig. 1b). It also refers to the temperature range where the mixture remains liquid (e.g., between compositions x_1 and x_2). Wu et al. further employed DES systems as a eutectic combination of Brønsted or Lewis bases and acids that comprise a variety of cationic/anionic species (Fig. 1c) [10].

The conventional classifications of DESs are: 1) *Type I*: comprises a metal chloride and ammonium salt (quaternary), 2) *Type II*: contains a metal chloride (hydrate) and ammonium salt (quaternary), 3) *Type III*: combines HBD (e.g., a polyol, carboxylic acid, or an amide) and a ammonium salt (quaternary), 4) *Type IV*: involving HBD and a metal chloride hydrate [24], and 5) *Type V*: consists of HBDs, molecular HBAs and nonionic components [11]. Fig. 2 shows the various HBDs employed for DESs application [24].

3. The DES preparation approaches

A chemical compound is created by one or more reactions between two or more reactants, which result in the creation of a product. The synthesis methods of DESs are a simple mixing of HBD and HBA components. Hence, DESs are not synthesized instead they are prepared by mixing and they don't involve any chemical reaction [23]. Fig. 3 Summarizes the various DES preparation approaches [45].

3.1. Heating and stirring methods

DESs can be prepared using a simple heating and stirring approach. Hence, DES preparation is a simple, cost-effective,

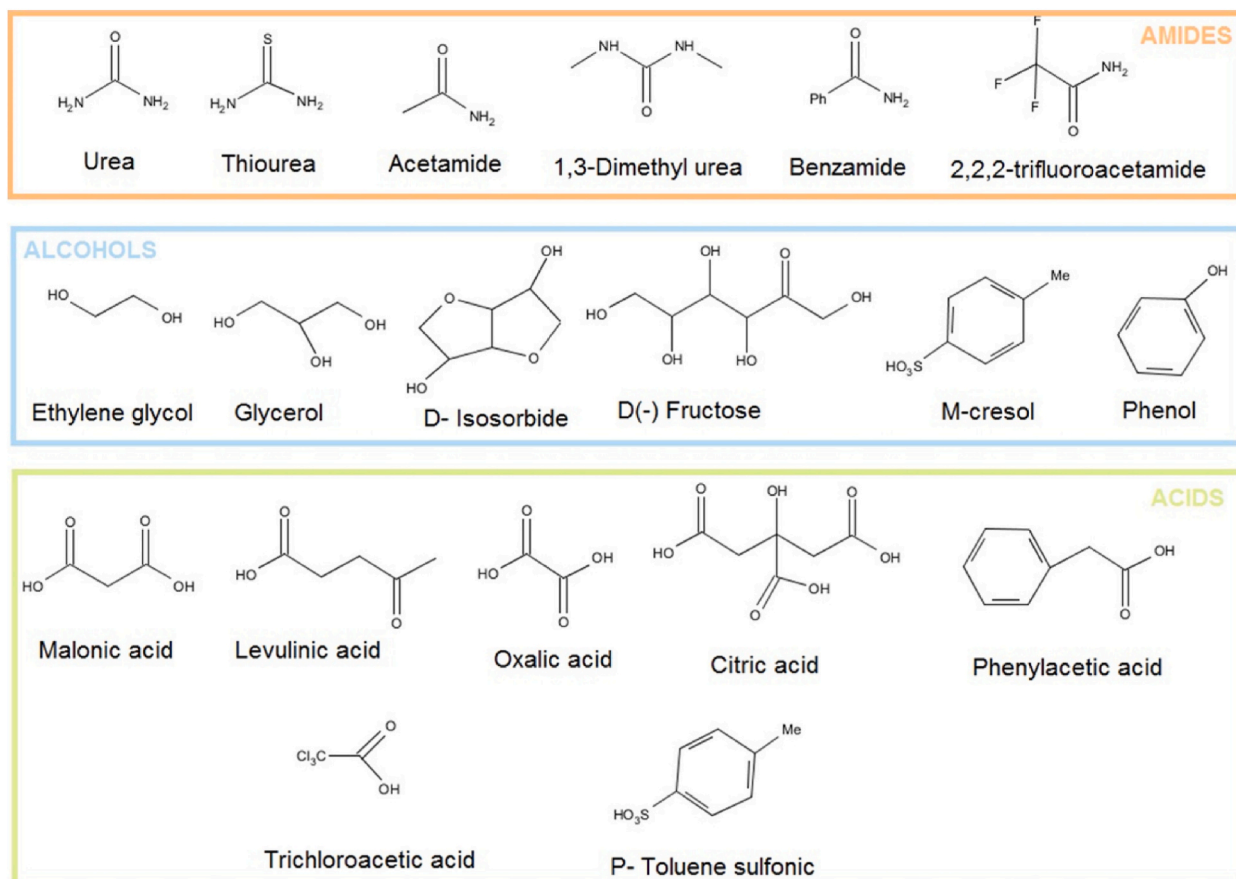


Fig. 2. The various HBDs employed for DESs. Reproduced in permission from Ref. [24].

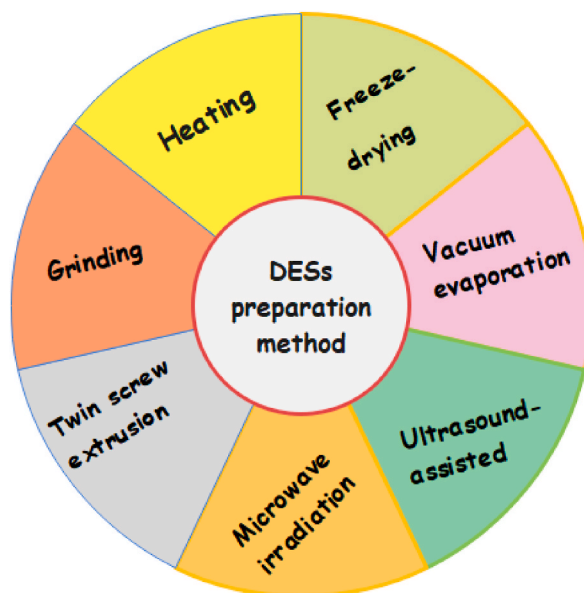


Fig. 3. Schematic representation of DES preparation methods.

environmentally compatible, and no-waste or by-product formation approach [7,25]. Different reports have used temperature values ranging from as small as ambient temperature to as large as 130 °C for up to a few hours based on the boiling point, stability, and melting point of the reagents [26]. However, some restrictions have to be taken into account before using these approaches in the DES preparation. Gurkan et al. showed the formation of crystals when HBA (*i.e.* $[\text{Ch}^+][\text{Cl}^-]$) was blended with ethylene glycol (EG) [27]. The crystal formation is obtained at very low temperatures and/or very short heating and stirring times [27]. Rodriguez et al. also showed that employing high temperatures for a long time leads to decomposition and by-product formation [28]. Hence, for DES preparation, knowing the appropriate stirring time and temperature is vital to attain the appropriate homogenization of the entire components (Table 1) [27].

3.2. Freeze-drying approach

It involves the addition of HBD and HBA in stoichiometric amounts and then distilled water dilution to attain about a 5 % aqueous solution (frozen at 77 K or 253 K, *i.e.*, very low temperature), followed by lyophilization freeze-dried to attain a clear viscous liquid [39,40]. The freeze-drying approach permits the organic self-assembly incorporation of microorganisms, big unilamellar vesicles of liposomes, and polymers based on proteins in DESs [40]. The water presence is important for the liposome formation. The direct mixing of neat DESs with an aqueous solution of liposomes can lead to a solution (aqueous) of both DES components. Moreover, the freeze-drying approach permits the integration of vesicles and micelles in DESs, that can act as capsules and nanoreactors, and leads to the applications of DESs in pharmaceutical and biological areas [39].

3.3. Vacuum evaporation approach

In this approach, the HBD and HBA are liquefied in water, and then the water evaporates by at 50 °C (rotary evaporation) to

Table 1
The various DESs and their components that have been prepared using a heating preparation approach.

Year	DES	Preparation method	Ref.
2020	Ethylammonium chloride/glycerol/ ZnCl_2	Direct mixing and then stirring at 70 °C	[29]
2020	$\text{Zn}(\text{ClO}_4)_2 \cdot 6\text{H}_2\text{O}$ /succinonitrile	Direct mixing followed by stirring (80 °C)	[30]
2020	Lithium salt/amide-based DES	Direct mixing and then stirring at 100 °C	[31]
2021	LiClO_4 /Urea	Direct mixing and then string at 60 °C for 2 h	[32]
2021	Zinc triflate/EG	Direct mixing and then stirring at 60 °C	[33]
2022	Choline chloride/urea	Direct mixing after that stirring at 80 °C	[34]
2023	$\text{Zn}(\text{NO}_3)_2 \cdot 6\text{H}_2\text{O}$ /glycerol	Direct mixing and then stirring (90 °C)	[5]
2023	ZnCl_2 /urea	Direct mixing followed by stirring at 70 °C	[35]
2024	$\text{Zn}(\text{NO}_3)_2 \cdot 6\text{H}_2\text{O}$ /EG	Direct mixing and then stirring (90 °C)	[36]
2024	$\text{Zn}(\text{NO}_3)_2 \cdot 6\text{H}_2\text{O}$ /urea/EG	Direct mixing and then stirring (90 °C)	[37]
2024	ChCl /EG	Direct mixing after that stirring at 80 °C	[38]

produce the DES [41–43]. Dai et al. used this method for the formulation of natural DESs [43]. Natural DESs comprise of natural compounds, specifically metabolites (primary) like sugars, amino acids and organic acids [44]. The liquid obtained after evaporating the water is then dried out inside a desiccator that contains a silica gel till a constant weight is attained [42]. This approach employs a comparatively smaller temperature in comparison with the stirring and heating approach. Moreover, the vacuum evaporation approach is appropriate for the synthesis of natural DES as utmost natural compounds employed in their synthesis attain high melting point values [43] and the constituents should be soluble in water to use this approach.

3.4. Grinding method

Florindo et al. used the grinding approach to make DESs without the employ of heat, as presented in Fig. 4 [45]. This approach comprises the mixing of HBD and HBA components followed by grinding with mortar and pestle at ambient temperature until a mixture (homogenous) was attained [45,46]. Then, for moisture removal, the HBA $[\text{Ch}^+][\text{Cl}^-]$ is initially dried in a vacuum oven for two days at 40 °C and followed by maintaining under high vacuum in a Schlenk for about 4 days because of its hygroscopic characteristics. The grinding approach was compared with the heating/stirring approach and used to analyze the DES purity [45].

3.5. Twin screw extrusion approach

The twin-screw extruder (TSE) mechanochemical preparation by grinding two or more solid reagents together has been used to eliminate/reduce the use of toxic substances and hazardous materials in material processing and chemical synthesis [47]. Crawford et al. employed this technique for large-scale synthesis of DESs to settle out the limitations of the heating/stirring approach [48]. The DES is synthesized by preheating the entire sections of TSE and then adding mixing the HBD and HBA (*i.e.* stoichiometric ratios) into a feed port. The TSE approach is important as it is easily scalable and allows high throughput production, an effective and continuous route for DES synthesis, owns short heat exposure times, no thermal degradation, and a simple collection of exceedingly viscous DESs inside the containers. In general, this approach overcomes the problems in moving the end product from the reactor to final storage vessels frequently met by other synthesis approaches [48].

3.6. Microwave irradiation approach

Gomez et al. studied the microwave-aided synthesis of DESs [49]. This approach reduces the energy cost and time of DES synthesis and creates an exceedingly eco-friendly synthesis method [50,51]. In this approach, a mixture of HBD/HBA was put in a vial of 20 mL, followed by irradiation with a microwave for about 20 s. This approach decreases the time of preparation from many hrs. to about 20 s and needs 650 times less energy than the heating and stirring approach [49]. This technique is generally a cheaper, greener, faster, and easier route for the preparation of DESs than conventional methods [50]. However, the combinations of HBD and HBA have to be judiciously nominated and heating time and power (*i.e.*, experimental factors) must be optimized carefully to avoid side reactions.

3.7. Ultrasound-assisted preparation

Ultrasonic waves can also be used in the synthesis of DESs [52,53]. In this approach, HBD and HBA in stoichiometric amounts were mixed in a vial of glass. Then the vial was sealed and put for 1–5 h inside an ultrasonic bath, and depending on the DES constituents, the temperature is controlled from ambient temperature to 60 °C. After that, the prepared DESs were placed for about 24 h in a similar vial at room temperature to confirm the creation of a homogenous mixture. The prepared DESs using this approach are not prone to crystallization and are stable over time, even after many days [53]. Furthermore, similar physicochemical properties like viscosity,



Fig. 4. Schematic representation of DES preparation using the grinding method. Reproduced with permission from Ref. [45].

FT-IR spectra, decomposition temperature, and density have been detected in DESs obtained by both ultrasonic aides and heating/-stirring approaches [50].

4. Physicochemical properties

4.1. Freezing point/melting point

The DESs freezing points are usually smaller than the individual components. For instance, the freezing point of Urea/ChCl (2:1) equals 12 °C noticeably smaller than the melting point of that of urea (133 °C) and ChCl (302 °C) [22]. The ratio (molar) of salt: HBD influences the DESs freezing points. Nevertheless, there is no clear correlation between the DESs freezing points and melting points of individual units. Smith et al. reported that the DES freezing point influenced by the magnitude of the interactions of HBD and halide ions, energy (lattice) of DES, and changes in entropy [54]. DESs having melting points under 50 °C are more attractive even though all DESs studied have freezing points under 150 °C [55]. The freezing point of DES depends on the hydrogen bonding (interaction strength) of the HBD with organic salt anion. The DES together with urea that formed from the salt of choline has a freezing point increasing in the order of $\text{BF}_4^- < \text{Cl}^- < \text{NO}_3^- < \text{F}^-$. NMR spectra showed the occurrence of hydrogen bonding inside the eutectic mixtures [56].

4.2. Density

It is a vital characteristic for knowing the miscibility and solvent diffusion of DESs [57]. In general, a specific gravity meter is used to determine the density of DESs [58]. The density of ZnCl_2 -acetamide (1: 4) DES is 1.63 g/cm³ while the density of ZnCl_2 -urea (1:3:5) DES is 1.36 g/cm³. This density difference could be ascribed to the packing of the DES and different molecular organizations. The densities of both DESs are larger than the pure HBDs *i.e.*, urea: 1.32 g/cm³ acetamide: 1.16 g/cm³. This can be explained with the theory of hole that employs the empty holes or vacancies DESs and their size determines their density [59]. The hole theory clarifies the enhanced density of DES by a reduction of the radius of the hole (average) by mixing two constituents [55].

4.3. Viscosity

The small value of viscosity is important in electrochemical systems in DESs because it offers the ionic species free mobility owing to the creation of hydrogen bonds (weak intermolecular) between compounds of HBA/HBDs [5,60]. The large value of viscosity for DESs is frequently ascribed to the occurrence of an extensive hydrogen bonds (network) between HBA and HBD constituents and results in a free species with lower mobility within the DES [5]. The tiny void volume and big ion size of most DESs along with van der Waals or electrostatic interactions can contribute to the large viscosity value of DES. The formulation of DESs with low viscosity values is extremely desirable due to their possible employment as green media. In general, eutectic mixture viscosities are chiefly influenced by the DES components' chemical nature such as the type of HBDs and the ammonium salts, HBD molar ratio/organic salt, water content, and the temperature [25]. The viscosity of DES is additionally influenced by the free volume and the hole theory can also be employed to design low viscosities DESs. For example, the employment of hydrogen-bond donors (fluorinated) or small cations can lead to the creation of low-viscosity DES [61].

4.4. Ionic conductivity (σ)

It is a notable transport characteristic of DESs in the use of electrochemicals (*e.g.*, electrolytes for redox-flow batteries) [11]. The σ is influenced by temperature, viscosity, ion mobility and charge carriers (concentration) [5]. It is also strongly correlated with viscosity *i.e.* the viscosity value increases as the σ decreases. Most DESs possess poor σ (<2 mS/cm), due to the relatively high viscosity values which may create a problem for some electrochemical applications [62]. DESs with low-viscosity possess large σ values because of the ionic species' free mobility as the hole mobility is enhanced. For instance, the lower viscosity value of ammonium-based DESs possesses a higher σ than phosphonium-based DESs [63,64]. In addition, the free volume of DESs can be enlarged by decreasing the size of the ions which can lead to a reduction in the viscosity values and a rise in the σ values [11]. The ammonium-based DESs with smaller sizes possessed a higher σ than the phosphonium-based DES, resulting in suitable electrolytes and solvents in electrolysis [64]. The relationship among temperature, viscosity and σ can be governed by the Walden rule. However, as these σ values depend on temperature, the σ can be forecasted by considering Arrhenius-type behavior. Abbott et al. reported σ of the ChCl-urea DES for the first-time measurement and revealed that σ significantly enhanced with increasing temperature [22]. Ghareh Bagh et al. also studied the σ profiles of sixteen DESs and saw a reliable tendency of increasing σ with temperature, which might be ascribed to the migration rate and higher kinetic energy of the molecules at the elevated temperature [65]. Moreover, Zhang et al. presented the increase in σ of DESs with increasing concentrations of salt (*e.g.*, EG-ChCl) [66]. However, this property is not working for all DESs, as the σ change is dependent on both the nature of salt and HBD nature (*e.g.*, tetrabutylammonium chloride (TBAC)-EG mixture) [57,60,67].

4.5. Surface tension

It is a measure of the energy needed to enhance the material's surface area. It is connected to the material tendency of a to possess the minimum possible surface area [58]. It is exceedingly reliant on the intermolecular force strengths between the salt and HBDs.

DESs with highly viscous are fluids with large surface tension [11]. The hydroxyl groups available in the cation result in a higher surface tension due to the hydrogen-bonding. The results of tetra propyl and tetra butyl ammonium DESs indicate that the increase in the cation alkyl chain length results in a higher surface tension [60]. According to Equation (1), the surface tensions linearly reduce with an increase in temperature and decrease with the increase in mole fraction of salt due to the weakening of the hydrogen bond in the HBD network by mixing [58], [68]. Many methods like the Wilhelmy plate [69], Du Nouy ring [70], and pendant drop [71] can be employed to measure the surface tension.

$$\gamma = a + b (T). \quad \text{Equation 1}$$

where T (K) is the temperature, a and b are constants, and γ (mNm^{-1}) is the surface tension.

4.6. Refractive index (n)

It is a unitless material property that measures the changes in the speed of light as it crosses in a medium (v) in connection to the speed of light in a vacuum (c) and according to Snell's law, it can be related as in equation (2) [11]. It can also be employed to measure the molecule's electronic polarizability and can offer valuable information in studying the molecular forces or solution behavior [45].

$$n = \frac{c}{v}. \quad \text{equation 2}$$

At several molar ratios (1:1.5, 2:1, and 3:1), the refractive indices of glycerol and ChCl were studied as a function of temperature. Kučan et al. discovered that the eutectic ratio had the greatest refractive index between 15 and 55 °C [11]. Another study by Hong-Zhen et al. showed the dependence of refractive index on the kind of HBD in DES by studying many DESs with varying amounts of HBDs in the same amount of HBA (*i.e.* tetrabutylammonium chloride (TBAC)) [72]. Amongst the HBDs studied, a DES made of phenylacetic acid (PAA) and TBAC with a molar ratio of 2:1 possessed the largest refractive index than propionic acid (PA) and TBAC with a molar ratio of 2: 1. A phenyl versus methyl group adhered to the carboxylic acid in the structure of HBD separates the two DESs composed of PAA and PA HBDs. The trend of refractive index, which was supported by the measurement of viscosity in a related study, indicated a greater degree of association of bulkier PAA with other molecules of PAA. The n can also be used to look into a DES's electrical properties. The experimental n values for betaine and L-proline-based DES were employed to determine the molar refractivity (Equation (3)) by Sanchez et al. [73]. They showed that the molar refractivity was discovered to be dependent on the composition and fraction (molar) of HBD and independent of temperature.

$$R_m = ((n_D^2 - 1)) / ((n_D^2 + 1))V. \quad \text{Equation 3}$$

Therefore, the DES n can be an important tool in supplementing the measurements of physical characteristics as an additional support to the formation of hydrogen bonds.

4.7. Stability

DESs possess good thermal and chemical stability and they are not combustible [60]. Thermogravimetric analysis techniques are employed to study DES's thermal stability [74]. The DESs with higher decomposition temperatures indicate good stability DES and can be used at higher temperatures [75]. The DES stability depends on the molar ratio, heating time, composition, number of HBA/HBD groups as well as the functional groups and spatial structure. DESs that possess a structure with a high carboxyl (-COOH) group are more stable [25]. The formation and stability of hydrogen bonds can be determined by their three-dimensional structure and the amount of hydrogen bond groups [75].

4.8. pH

It is a scale used to quantify the solution acidity. It is also a vital component in the creation of DESs. As previously mentioned, DESs can be defined as a system that is built up with group of Lewis bases and acids, with the pH of the system being a crucial factor [10]. The pH values are determined by the relative acidity of the joint anionic/cationic species. A mixture's acidity plays a key role in determining the other characteristics of the system and will be crucial in future industrial applications. Because of worries about the kinetics of chemical reactions and corrosion, the pH is significant when choosing piping material in industrial processes [11]. A report of pH values in a series of DES mixture tests of D-glucose with ChCl at various molar concentrations was conducted by Hayyan et al. [76]. They observed a pH value of 7 (neutral mixture) in 25–45 °C temperature range, showing the possibility of using this mixture at the industrial scale. Nevertheless, in the temperature ranges of 25–85 °C, a small dependence of pH (linear) with enhancing temperature was detected. This type of behavior of linear reduction in pH with an enhancement in temperature was observed by Skulcova et al. [77]. This kind of relationship held for mixtures of various DES and observed a substantial difference in the values of pH depending on the HBD employed.

5. Detection strategies

5.1. Fourier transform infrared spectroscopy (FTIR)

It is an approach employed to study the various molecular structures using infrared spectrum emissions of samples over a long range of wavelengths [5,11,78]. FTIR is an important device for obtaining accurate data on DES compound structure. It is one of the first methods that has been used to detect what might be available in the sample. FTIR is a crucial method for identifying potential contaminants in a material. Nonetheless, its primary use is to detect the change in molecular structures and make necessary adjustments when each component of DES is combined at varying concentrations. For example, FTIR was employed to determine the solvent formation structure of DES from citric acid and ChCl. Additionally, Ibrahim et al. studied the structures of DES from EG and different salts using FTIR to determine whether any new functional groups were present in the DES structures [58]. Additionally, FTIR was employed to study the existence of eutectic mixes between choline and other compounds and to explain the structural alterations present in the DESs at different temperatures [78].

5.2. Raman spectroscopy (RS)

It is employed to check the vibrations and molecular rotations in a system and other low-frequency modes as well [58]. It functions by transmitting monochromatic light over a sample and detecting the transitions between elastic/inelastic scattering at specific wavelengths. This allows for the identification of various compounds. It is utilized to ascertain what is contained in the DES sample, how it is contained, and how to use it to take advantage of different approaches [78]. Because of these properties, RS is often employed in conjunction with FTIR, and Nuclear magnetic resonance spectroscopy to approve the purity and composition of the studied substances [79].

5.3. Thermogravimetric analysis (TGA)

It is used to examine the mass change (physical) versus time/temperature. It allows some chemical and physical characteristics to be inferred [80]. However, as physical properties and thermal behavior are frequently closely correlated, it can also detect marked changes and deviations in property due to phase change [78]. This technique is often applied in determining the change in characteristics because of thermal events like desorption, absorption, vaporization, decomposition, reduction sublimation, and, oxidation [11].

5.4. Differential scanning calorimetry (DSC)

It is a thermo-analytical method that helps in knowing the heat needed to get the detected change in temperature a sample. It is also important in scrutinizing heat (latent) through transformation events like phase changes/glass transitions [58]. This method is usually employed in identifying enthalpies of formation and fusion, thermal stability, melting points, and heat capacity data for both pure constituents and mixtures of DESs [78]. DSC can capture phase change events and is a useful tool in detecting anomalous characteristics in DES. Morrison et al. obtained a DSC curve for ChCl to malonic acid with a 1:1 M ratio and exhibited no peaks related to glass-transition, melting, or crystallization instead they demonstrated a baseline shift ascribed to the inability of DES to nucleate [81, 82]. However, Francisco et al. presented numerous natural DES that showed only glass transitions [83].

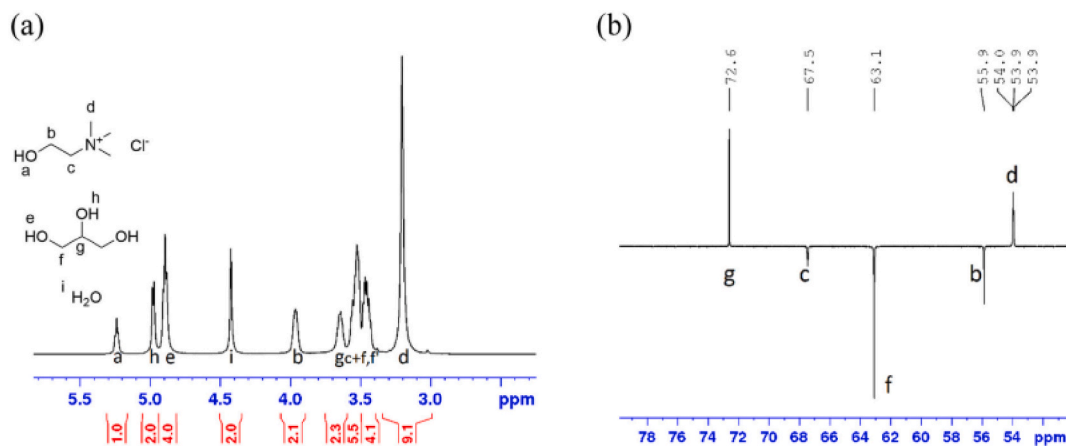


Fig. 5. The spectra of W: Gly: ChCl at 298 K. ¹H NMR (a) and ¹³C NMR (b). Reproduced with permission from Ref. [84]. Copyright 2019, Journal of Elsevier.

5.5. Nuclear magnetic resonance spectroscopy (NMR)

The NMR analysis is used to study the structural/compositional study in DES [84]. The NMR helps in verifying/quantifying what exists in materials before doing other analytical methods and allows to make decisions using the evidence of subtle shifts, water content, and impurities in functional groups [85]. Therefore, NMR is a great tool to obtain a baseline in understanding what functional groups are available and how they interact and rearrange within a structure. The NMR helps in studying composition and transport phenomena analysis in DES but labeling molecular level may be needed to attain discovery of a nucleus [11]. For instance, I. Delso et al. studied numerous NMR spectroscopic methods to determine the structure (molecular) of the ternary DESs made of urea (U), choline chloride (ChCl), or EG or glycerol (Gly), and/or water (W), as presented in Fig. 5a and b [84].

5.6. Fluorescence spectroscopy (FS)

It is multi-dimensional and many parameters characterize polarization in steady-state emission and excitation wavelengths, quantum yield, anisotropy, rotational reorientation time, and excited-state lifetime [86]. It is a vital tool for studying the structure, micro environmental polarity, solvation, and interactions within DESs. Pandey and co-workers studied the region of cybotactic that surrounds solvato chromic fluorescent probes and the local micro-environment that dissolved in DESs. The Pandey group, in their first contribution, studied the polarity in ethaline, reline, glyceline and maloline with a 2:1 M ratio of malonic acid: ChCl based on a suite of the sensitive polarity fluorescent reporters (pyrene-1-carboxaldehyde, p-toluidinyl-6-naphthalenesulfonate, pyrene, 1-anilino-naphthalenesulfonate, 6-propionyl (dimethylaminonaphthalene), coumarin 153 and Nile Red) [87]. Pandey and co-workers in their subsequent work studied cosolvent effects such as tetra- EG Ref. [88], water [89], solute (e.g., LiCl [90], 2, 2, 2-trifluoroethanol and hexamethyl phosphoramidate [91], or modification on DES systems.

5.7. Broadband dielectric spectroscopy (BDS)

It is a multipurpose method for studying the ionic and dipolar dynamics by the material polarization response at the applied oscillating electric field [92]. The information that obtains from BDS can permit in correlation of microscopic mechanisms to macroscopic physical characteristics like ionic conductivity, viscosity, surface tension, and eutectic composition that are essential in more general framework development for understanding DES systems [11,93].

5.8. Cyclic voltammetry measurements (CV)

It is the widely employed approach for getting qualitative data about the electrochemical characteristics of DES solvents [94]. It gives a redox potential rapid location of the electroactive species. In a CV analysis, a time-varying potential is applied continuously to the working electrode [5]. Initially, the potential sweep is done in one direction, and then inverted, and the cycle can be repeated many times. The decrease or increases in potential values in reduction or oxidation reactions that may happen at the material surface are studied and result in faradaic currents that appear as reduction or oxidation peaks on the voltammogram [94]. The faradaic current depends on the active species mass transfer and the kinetics movement [11]. Moreover, a capacitive current can be detected as a result of the possible adsorption of chemical species and double-layer charging of the electrochemically active surface [95]. In general, the various DES characterization approaches are summarized and presented in Fig. 6 [11,45,78,96].

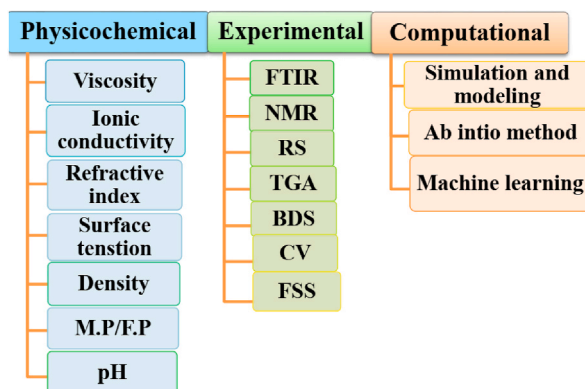


Fig. 6. Schematic representation of the various DES characterization approaches. Modified from Refs. [11,45,78,96].

6. Computational studies

6.1. Simulation and modeling

Computational approaches were recognized as a strong tool for analyzing systems of liquid (complex) even before curiosity in DESs attained popularity [97]. The simulation approaches were first employed for ILs by Hanke et al. in 2001 to minimize the energy and to replicate crystal structures using molecular dynamics and they performed simple methyl alkyl imidazolium salt structure analyses [98]. Rimsza et al. performed many DES-explicit simulations in 2012 that emphasized on optimization of energy for complexes of copper in reline [99], and then Sun et al. studied structural characteristics of reline later [100]. Introducing the computational approaches to the DES system allows cautious attention of the subtle variation that distinguishes the two sets, and needs various considerations and assumptions to be considered. Knowing what causes the sole characteristics of DESs is a complicated problem that is exclusively challenging to highlight and model the interest in considering DESs and ILs separately. This allows the existing computational approaches to be well matched to tackling these central problems and the majority of complications originate from the variety of DESs that may be employed; the variation of constituents forms a multiplicity of problems for simulation to address for the 4 classes of DESs [59], complex and varied hydrogen bond networks [101], mixed neutral and ionic species slow/glassy system dynamics and varying hydration effects [102].

6.2. Ab initio methods

To study the depression of the melting point at the DES eutectic composition important computational efforts have been done along with conventional experimental approaches. A core idea in DES is that the neutral species acts as the minor anionic classes complexing agent based on equation $[A]^- + xB \rightleftharpoons [A(B)_x]^-$ in which the charge (negative) is delocalized from the anion [11,101]. Delocalization of charge via the network of hydrogen bonds is considered to exist in the de facto decisions regarding the behavior of DESs. It is also one of the parameters accountable for the smaller DESs melting temperatures. Using ab initio simulations, the main emphasis of computational studies was on electronic conformations and energy minimization of the DES species.

Ab initio simulation: To estimate the essential characteristics of molecules, like conformational energies and electron cloud shapes, one must repeatedly solve the electronic Schrodinger equation. Using this method, Zahn et al. investigated a reline to confirm

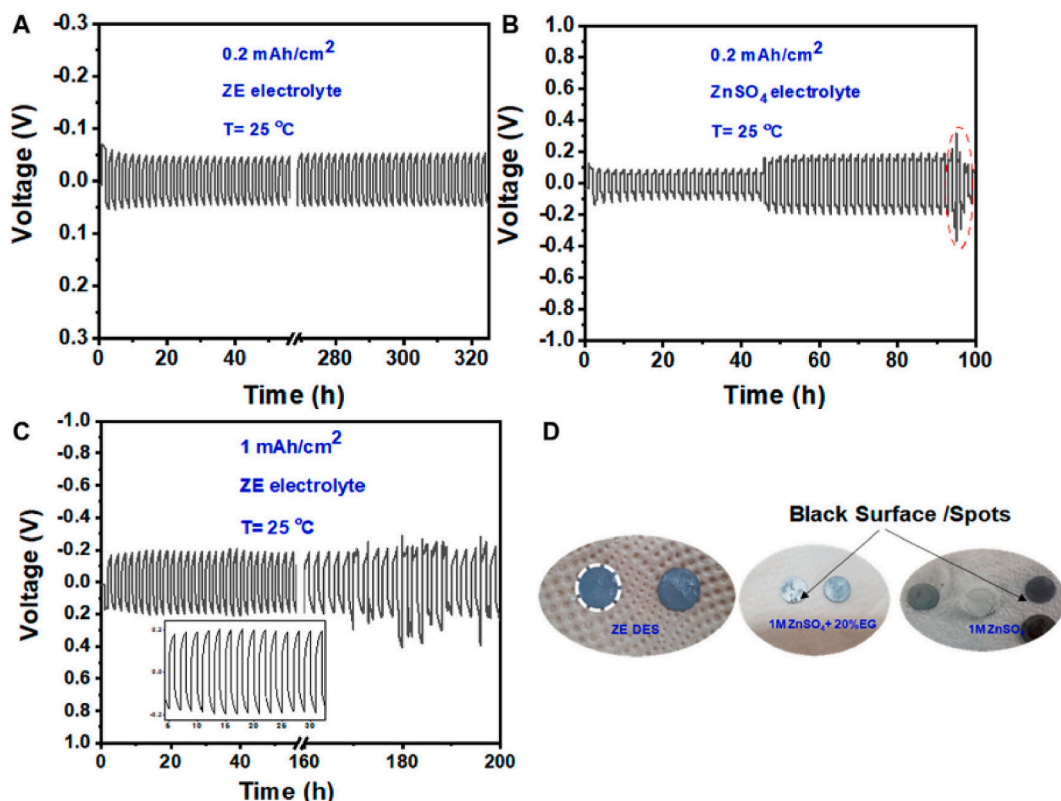


Fig. 7. The long-term plating/stripping recital of the anode (Zn metal) at 0.2 mA h cm⁻² in (a) EG/ZnCl₂ electrolyte (b) The aqueous ZnSO₄ (1 M) (C) at 1 mA h cm⁻² for EG/ZnCl₂ electrolyte. (d) Photographs image of the Zn foil attained at 0.2 mA h cm⁻² and after 50 cycles. Reproduced in permission from Ref. [111].

the minimal charge transfer amid the donor (hydrogen bond) molecule and the chloride ion. In reline, the donating cation of choline and the anion of chloride mainly maintain a close relationship [103]. The prevalent idea states that the anion of chloride split fully in the DES, which is not supported by this data. The advantage of “esoteric” hydrogen bonds was demonstrated by Hunt et al. in their report on ab initio studies. They also showed that the implicit of a neutral H-bonds network assumptions may not be true, and the simulations revealed that doubly ionic (ionic) hydrogen bonds were common in the systems under study [104]. Analogous investigations by ab initio approaches to predict the optimal geometries of urea dimers, EG dimers, ChCl, and malonic acid dimers were reported by Wagle et al. [105].

6.3. Machine learning

The machine learning basic principle is to employ algorithms to analyze and learn from data, and then to make predictions and decisions about the events in the real world [92]. Algorithms-based applications (research) have become progressively pervasive and extremely entrenched constituents of current knowledge, and machine learning has contributed important advances in different areas [106,107]. It is also a known new approach that leverages large data sets and computational power to attain notable results without the large cost of Ab initio molecular dynamics simulation [11]. For instance, by considering DES the future research works can be taken from two viewpoints: (1) In machine learning (basic research) would be employed to discover the structure of DESs in networks of hydrogen-bonding and to design novel DESs created using several non-covalent interactions of chalcogen bonding and halogen; (2) in application research the solvent systems would be designed based on the characteristic behaviors required for practical application [105]. Models-based machine learning can correct some of the challenges that plague several common approximations in conventional computing [96]. Moreover, the electron-density-based solution and molecular dynamics studies offer novel means of discovering binary fluids [96,105,108,109].

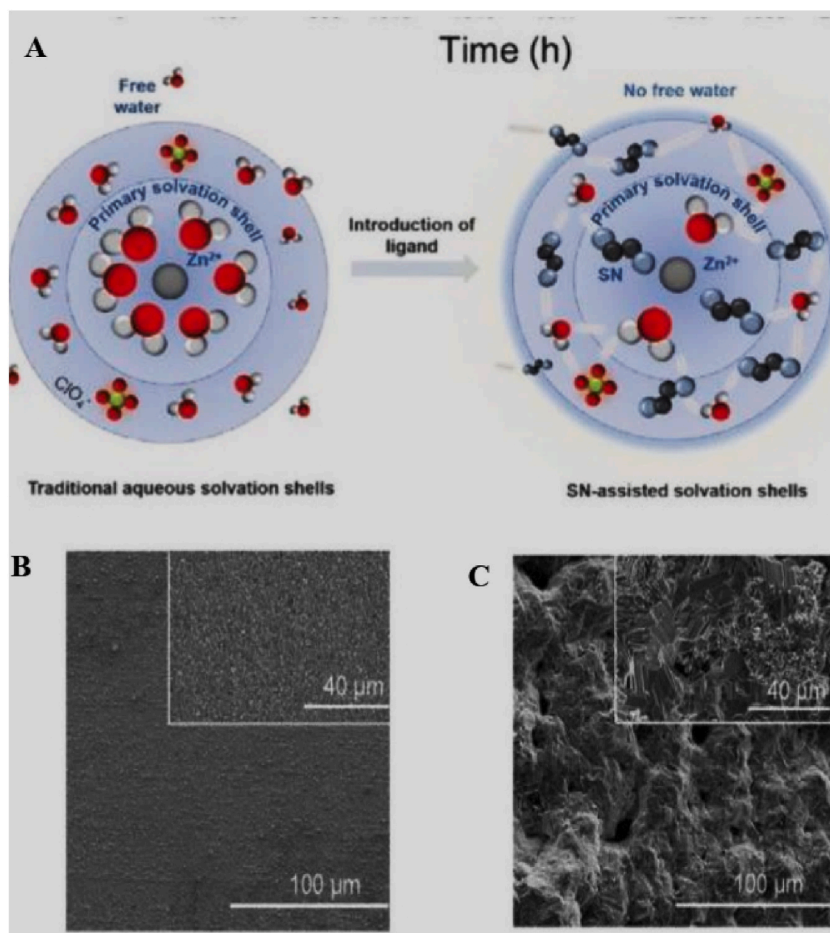


Fig. 8. Diagram representation of Zn^{2+} solvation structures in succinonitrile and aqueous-based Zn electrolytes (a). SEM images for Zn metal coated on the collector (stainless-steel) in succinonitrile (b) and $H_2O/Zn(ClO_4)_2 \cdot 6H_2O$ electrolytes (c). Reproduced in permission from Ref. [112].

7. Advances in DESs for ZABs

Currently, DESs have been broadly investigated for Zn batteries electrolytes due to their low toxicity, high stability in the moisture and air, high water-miscibility, low cost, and reversible and stable Zn stripping/plating with in cycling life improvement than the routine aqueous electrolytes [110]. A biocompatible, low-cost, and stable DES formed from $\text{ChCl}/\text{urea}/\text{ZnCl}_2$ for electrolyte was proposed by Kheawhom et al. [2]. They found that no dendrites were formed on the Zn metal surface showing the highly reversible stripping/plating property. Thorat et al. [111], also investigated the stability (reversibility) of Zn in the EG/ZnCl_2 DES electrolyte employing a Zn/Zn cell (symmetric) and the electrodes of Zn used as both negative and positive electrodes under galvanostatic situations. They indicated that the anode (Zn metal) with excellent performance was further confirmed through long-lasting cycling at various current densities, as presented in Fig. 7A. The cell (symmetric) functions steadily over 300 h (>180 cycles) and 0.25 mAh cm^{-2} , showing the large Zn anode reversibility. The curve (polarization) continued stable throughout the whole cycle process. In contrast, a gradual enhancement in overpotential values was detected for Zn/Zn (symmetric cells) cycled at about 0.25 mAh cm^{-2} in the traditional aqueous ZnSO_4 electrolyte. Zn stripping/plating would only be cycled at 0.25 mAh cm^{-2} for about 90 h in the aqueous ZnSO_4 electrolyte, as indicated in Fig. 7B. They opened the Zn/Zn cell with both $\text{ZnSO}_4/\text{EG}/\text{H}_2\text{O}$ and aqueous ZnSO_4 electrolytes at 0.2 mAh cm^{-2} and 50 cycles and obtained the Zn foil had black spots that could further grow and lead to death of the cell (Fig. 7D). On the other hand, the cell-cycled electrolyte of EG/ZnCl_2 showed no such spots (black) that indicate the high stability of the Zn anode in the EG/ZnCl_2 electrolyte. Hence, the Zn/Zn cell (symmetric) possessed very large stability for about 200 h with an overpotential value below 200 mV and at a large current density value of 1 mAh cm^{-2} (Fig. 7C).

The new group of the Zn electrolytes (hydrated eutectic) with an accurate level of hydration was made for battery (Zn-organic) by simple mixing of a neutral ligand of succinonitrile and a cheap hydrated salt ($\text{Zn}(\text{ClO}_4)_2 \cdot 6\text{H}_2\text{O}$) by Yang et al. [112]. Here, the Lewis basic succinonitrile participates in Zn^{2+} ions' primary solvation shell with the creation of $[\text{Zn}(\text{OH}_2)_x(\text{SN})_y]^{2+}$ (i.e. a complex of hydration-deficient cations). The molecules of water substituted by succinonitrile are bonded through succinonitrile in Zn^{2+} cations outer solvation shell and can contribute to the creation of the eutectic structure (hydrated), as presented in Fig. 8a. The SEM pictures showed that the Zn electrolyte allows Zn stripping/plating of dendrite-free system (Fig. 8b) while the Zn metal deposited on the stainless-steel surface is uneven with several holes and humps when aqueous electrolyte with $\text{H}_2\text{O}/\text{Zn}(\text{ClO}_4)_2 \cdot 6\text{H}_2\text{O}$ was used (Fig. 8c).

The plating/stripping characteristic of the electrolytes the Zn|Zn cell (symmetric) with zinc triflate ($\text{Zn}(\text{OTf})_2$) in water and EG with the optical picture of the separator (bottom) and Zn foil (top) and the micrograph SEM of the Zn foils with $\text{Zn}(\text{OTf})_2$ salt in water and EG was presented by Verma et al. [113]. They showed that 1 h deposition intervals (i.e. 0.5 mAh/cm^2 per half cycle) and current density of 0.5 mA/cm^2 , the $\text{Zn}(\text{OTf})_2/\text{EG}$ system would cycle for more than 600 h, or about 2.4 times longer than the system of $\text{Zn}(\text{OTf})_2/\text{water}$ (Fig. 9a). The overpotential of EG-based electrolytes is bigger than the water counterparts. However, the profiles of overpotential in the EG-based electrolytes remain smooth without large variations. On the contrary, the electrolytes based on water indicated exceedingly high overpotentials, and the reduced overpotentials to nearly zero showed a short-circuiting (Fig. 9a) [114]. Moreover, also analyzed the optical image of the separator and the Zn foil for $\text{Zn}(\text{OTf})_2/\text{EG}$ electrolyte was analyzed by Verma et al. (Fig. 9b). The SEM picture of Zn foil indicates that the deposition happens with morphology of granular structures (Fig. 9b). In contrast, the optical image of the cell cycle in water/ $\text{Zn}(\text{OTf})_2$ electrolyte indicates that Zn dendrites are growing and can even pierce the separator, as presented in Fig. 9c. The SEM picture of the Zn foil indicates that a platelike morphology rises on the Zn foil. The electrolytes based on EG alleviate the difficulties encountered in electrolytes based on water by decreasing the evolution of gas and electrolyte decomposition during the plating/stripping at the Zn metal anode in the assembled rechargeable ZABs [113,115]. Furthermore, DESs have been used in electrochemical systems, and there is rising demand in their ionic properties. Using highly conductive materials during electrolysis can reduce ohmic loss and cell voltage, resulting in larger efficiency of energy [116]. However, a significant limitation in the application of DESs both in electrochemistry and other research areas is their viscosity, which is strongly correlated with conductivity, higher viscosity generally results in reduced conductivity [5]. The compositions DES that display small viscosity, large σ , and excellent stability (electrochemical) possess necessary properties (physicochemical) as electrolytes, which greatly determine the electrochemical performance of ZABs [117]. Moreover, for recycling of battery, the DES viscosity has to be well controlled to enhance the efficiency (kinetics) [10].

8. Conclusion and outlooks

In summary, DESs have many unique advantages such as good stability in the moisture and air, low cost, low toxicity, nonvolatile, easy to prepare, and higher electrochemical and thermal stability than other electrolyte systems. The DES electrolytes with high concentration also enable the stabilization of interfaces of electrode and electrolytes which broadens electrochemical stability window (ESW) and hinders the creation of dendrite in ZABs. DES electrolytes are created when only the intermolecular interactions between constituents (i.e. HBD and HBA) are stronger than the individual constituents. One of the major problems in DES electrolytes is their inferior ionic conductivities and high viscosities at ambient temperature. The pioneering DES materials with optimized interactions in the intermolecular structure are exceedingly needed for the acceleration of ion migration by keeping the eutectic essence. For instance, the pairs of HBD/HBA with different substituents, functionalities, and compositions have to be explored. The versatile functionalities and types of DESs will open innovative paths for future environmental and energy applications and more theoretical and experimental works are needed. Hence, the DESs are promising electrolytes for creating safe and cheap energy storage materials.

Moreover, to increase the recital of the DES for ZABs the following issues have to be considered.

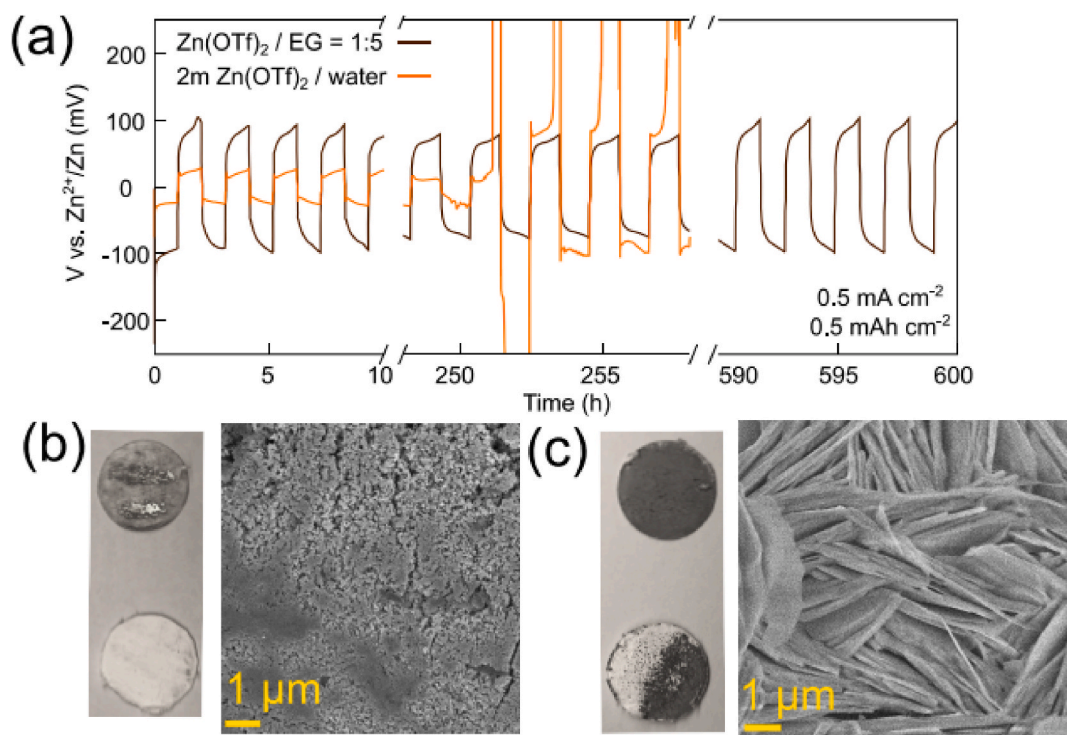


Fig. 9. The plating/stripping characteristics of the electrolytes in Zn|Zn cell (symmetric) with Zn(OTf)₂ in water and EG (a). The optical pictures of the separator (bottom) and Zn foil (top) and Zn foils SEM micrograph with salt of Zn(OTf)₂ in EG (b) and water (c). Reproduced in permission from Ref. [113].

(a) Optimization of viscosity: DESs are likely a predominant player in various industries despite their extremely high viscosities (a crucial property shared with ILs) as viscosity is an essential transport characteristic (e.g. species diffusion coefficients and electrolyte conductivity in the DES). Hence, much attempt has been employed to decrease the viscosity of DES. Moreover, there also are less comprehensive predictive models on DESs.

(b) Interphase chemistry: One of the most essential elements governing the rechargeable batteries cycling life is the surface chemistry of solid electrolyte interphase (SEI). Despite their relatively high redox potential, eutectic electrolytes are advantageous for Zn anode-related chemistry. For instance, a hybrid inorganic/organic SEI with rich in Zn fluoride-creates on the anode of Zn from the interaction of eutectic electrolyte (e.g. Zinc (II) bis(trifluoromethanesulfonyl)imide (Zn(TFSD)₂-acetamide), indicating a marked alter in the coordination of TFSI⁻ situation in the intrinsic network of ion-association in the current eutectic liquid. Overall, in RZBs the interphase chemistry would be synergistically controlled through the structure of solvation with low energy of dissociation and complex molecular structure with the interactions of H-bond in the eutectic electrolytes. This finally determine the stability and composition of eutectic electrolyte and electrode interphases by the effects of eutectic on deposition sequence and potential.

(c) Investigating the structure of DES: In-situ or ex-situ/operando characterizations as well as modeling (e.g. molecular dynamics (MD)) and computing (e.g. Discrete Fourier Transform, (DFT)) are used to examine the geometries of coordination and eutectic systems mechanisms at the molecular level. However, the specific qualities of DESs are a multidimensional challenge that is notably difficult to understand, emphasizing the necessity to treat DESs independently from ILs. The present computational approaches are employed to directly solve these main difficulties from the huge variety of potential DESs that would be prepared. This large variety of parts makes a multiplicity of problems for simulation to solve that comprises a minimum of five DES classes, complex and varied networks of hydrogen bonding, mixed neutral and ionic species, effects of varying hydration, and glassy/slow system dynamics. Despite these issues, few papers on computational studies of DES have been published. In this environment, more profound insights are required.

(d) Investigation of Supramolecular DESs (SUPRADESs): A new subclass of DESs with inclusion properties represents a recent discovery that could significantly influence the advancement of green chemistry. SUPRADES, as described in the literature, are composed of environmentally friendly components, and their physicochemical properties are comparable to those of conventional DESs. Furthermore, their supramolecular structure allows for selective binding of diverse chemical substances, resulting in significantly greater efficiency for numerous applications when compared to traditional DESs.

CRedit authorship contribution statement

Fentahun Adamu Getie: Writing – original draft, Investigation, Formal analysis, Conceptualization. **Delele Worku Ayele:** Supervision, Data curation, Conceptualization. **Nigus Gabbiye Habtu:** Investigation, Data curation, Conceptualization. **Temesgen Atnafu Yemata:** Writing – review & editing, Data curation, Conceptualization. **Fantahun Aklog Yihun:** Writing – review & editing. **Ababay Ketema Worku:** Writing – review & editing. **Minbale Admas Teshager:** Writing – review & editing.

Data availability statement

Data will be made available on request.

Declaration of competing interest

The authors declare no known competing financial interests that could have appeared to influence the work reported in this paper.

Acknowledgments

This work reported in this paper was supported by Bahir Dar Energy Center, Bahir Dar Institute of Technology, Bahir Dar University, Ethiopia.

References

- [1] F.A. Getie, D.W. Ayele, N.G. Habtu, F.A. Yihun, T.A. Yemata, Development of electrolytes for rechargeable zinc-air batteries: current progress, challenges, and future outlooks, *SN Appl. Sci.* 4 (2022), <https://doi.org/10.1007/s42452-022-05156-z>.
- [2] W. Kao-ian, R. Pornprasertsuk, P. Thamyongkit, T. Maiyalagan, S. Kheawhom, Rechargeable zinc-ion battery based on choline chloride-urea deep eutectic solvent, *J. Electrochem. Soc.* 166 (2019) A1063–A1069, <https://doi.org/10.1149/2.0641906jes>.
- [3] G. Ambissa Begaw, D. Worku Ayele, A. Ketema Worku, T. Alemneh Wubieneh, T. Atnafu Yemata, M. Dagneu Ambaw, Recent advances and challenges of cobalt-based materials as air cathodes in rechargeable Zn–air batteries, *Results Chem.* (2023) 100896, <https://doi.org/10.1016/J.RECHEM.2023.100896>.
- [4] S. Suren, S. Kheawhom, Development of a high energy density flexible zinc-air battery, *J. Electrochem. Soc.* 163 (2016) A846–A850, <https://doi.org/10.1149/2.0361606jes>.
- [5] F.A. Getie, D.W. Ayele, N.G. Habtu, F.A. Yihun, T.A. Yemata, M.D. Ambaw, A.K. Worku, Binary glycerol-based deep eutectic solvents containing zinc nitrate hexahydrate salt for rechargeable zinc air batteries applications with enhanced properties, *Heliyon* 9 (2023) e17810, <https://doi.org/10.1016/j.heliyon.2023.e17810>.
- [6] N.G. Habtu, A.K. Worku, D.W. Ayele, M.A. Teshager, Z.G. Workineh, Facile preparation and electrochemical investigations of copper-ion doped α -MnO₂ nanoparticles, *Lect. Notes Inst. Comput. Sci. Soc. Telecommun. Eng. LNICST* 412 (2022) 543–553, https://doi.org/10.1007/978-3-030-93712-6_36. LNICST.
- [7] Z.P. Cano, M.G. Park, D.U. Lee, J. Fu, H. Liu, M. Fowler, Z. Chen, New interpretation of the performance of nickel-based air electrodes for rechargeable zinc-air batteries, *J. Phys. Chem. C* 122 (2018) 20153–20166, <https://doi.org/10.1021/acs.jpcc.8b06243>.
- [8] Z. Liu, G. Pulletikurthi, A. Lahiri, T. Cui, F. Endres, Suppressing the dendritic growth of zinc in an ionic liquid containing cationic and anionic zinc complexes for battery applications, *Dalton Trans.* 45 (2016) 8089–8098, <https://doi.org/10.1039/c6dt00969g>.
- [9] M. Asmare Alemu, A. Ketema Worku, M. Zegeye Getie, Recent advancement of electrically rechargeable di-trivalent metal-air batteries for future mobility, *Results Chem.* 6 (2023) 101041, <https://doi.org/10.1016/J.RECHEM.2023.101041>.
- [10] J. Wu, Q. Liang, X. Yu, L. Qiu-Feng, L. Ma, X. Qin, G. Chen, B. Li, Deep eutectic solvents for boosting electrochemical energy storage and conversion: a review and perspective, *Adv. Funct. Mater.* 31 (2021) 1–25, <https://doi.org/10.1002/adfm.202011102>.
- [11] B.B. Hansen, S. Spittle, B. Chen, D. Poe, Y. Zhang, J.M. Klein, A. Horton, L. Adhikari, T. Zelovich, B.W. Doherty, B. Gurkan, E.J. Maginn, A. Ragauskas, M. Dadmun, T.A. Zawodzinski, G.A. Baker, M.E. Tuckerman, R.F. Savinell, J.R. Sangoro, Deep eutectic solvents: a review of fundamentals and applications, *Chem. Rev.* 121 (2021) 1232–1285, <https://doi.org/10.1021/acs.chemrev.0c00385>.
- [12] N.N. Nam, H.D.K. Do, K.T.L. Trinh, N.Y. Lee, Design strategy and application of deep eutectic solvents for green synthesis of nanomaterials, *Nanomaterials* 13 (2023), <https://doi.org/10.3390/nano13071164>.
- [13] F.A. Getie, D.W. Ayele, N.G. Habtu, F.A. Yihun, T.A. Yemata, M.D. Ambaw, A.K. Worku, Binary glycerol-based deep eutectic solvents containing zinc nitrate hexahydrate salt for rechargeable zinc air batteries applications with enhanced properties, *Heliyon* 9 (2023) e17810, <https://doi.org/10.1016/j.heliyon.2023.e17810>.
- [14] K. Melethil, M.S. Kumar, C.M. Wu, H.H. Shen, B. Vedhanarayanan, T.W. Lin, Recent progress of 2D layered materials in water-in-salt/deep eutectic solvent-based liquid electrolytes for supercapacitors, *Nanomaterials* 13 (2023), <https://doi.org/10.3390/nano13071257>.
- [15] X. Peng, Z. Taie, J. Liu, Y. Zhang, X. Peng, Y.N. Regmi, J.C. Fornaciari, C. Capuano, D. Binny, N.N. Kariuki, D.J. Myers, M.C. Scott, A.Z. Weber, N. Danilovic, Hierarchical electrode design of highly efficient and stable unitized regenerative fuel cells (URFCs) for long-term energy storage, *Energy Environ. Sci.* 13 (2020) 4872–4881, <https://doi.org/10.1039/d0ee03244a>.
- [16] K.A. Pishro, M.H. Gonzalez, Use of deep eutectic solvents in environmentally-friendly dye-sensitized solar cells and their physicochemical properties: a brief review, *RSC Adv.* 14 (2024) 14480–14504, <https://doi.org/10.1039/d4ra01610f>.
- [17] X. Ge, C. Gu, X. Wang, J. Tu, Deep eutectic solvents (DESS)-derived advanced functional materials for energy and environmental applications: challenges, opportunities, and future vision, *J. Mater. Chem. A* 5 (2017) 8209–8229, <https://doi.org/10.1039/c7ta01659j>.
- [18] M. Vilková, J. Plotka-Wasyłka, V. Andruch, The role of water in deep eutectic solvent-base extraction, *J. Mol. Liq.* 304 (2020), <https://doi.org/10.1016/j.molliq.2020.112747>.
- [19] A.K. Worku, D.W. Ayele, N.G. Habtu, M.D. Ambaw, Engineering nanostructured Ag doped α -MnO₂ electrocatalyst for highly efficient rechargeable zinc-air batteries, *Heliyon* 8 (2022) e10960, <https://doi.org/10.1016/j.heliyon.2022.e10960>.
- [20] C. Zhang, L. Zhang, G. Yu, Eutectic electrolytes as a promising platform for next-generation electrochemical energy storage, *Acc. Chem. Res.* 53 (2020) 1648–1659, <https://doi.org/10.1021/acs.accounts.0c00360>.
- [21] A.F. Alem, A.K. Worku, D.W. Ayele, N.G. Habtu, M.D. Ambaw, T.A. Yemata, Enhancing pseudocapacitive properties of cobalt oxide hierarchical nanostructures via iron doping, *Heliyon* 9 (2023) e13817, <https://doi.org/10.1016/J.HELIYON.2023.E13817>.
- [22] A.P. Abbott, G. Capper, D.L. Davies, R.K. Rasheed, V. Tambyrajah, Novel solvent properties of choline chloride/urea mixtures, *Chem. Commun.* (2003) 70–71, <https://doi.org/10.1039/b210714g>.
- [23] A.P. Abbott, D. Boothby, G. Capper, D.L. Davies, R.K. Rasheed, Deep Eutectic Solvents formed between choline chloride and carboxylic acids: versatile alternatives to ionic liquids, *J. Am. Chem. Soc.* 126 (2004) 9142–9147, <https://doi.org/10.1021/ja048266j>.

- [24] A.R. Mainar, E. Iruiñ, L.C. Colmenares, A. Kvasha, I. de Meazza, M. Bengoechea, O. Leonet, I. Boyano, Z. Zhang, J.A. Blazquez, An overview of progress in electrolytes for secondary zinc-air batteries and other storage systems based on zinc, *J. Energy Storage* 15 (2018) 304–328, <https://doi.org/10.1016/j.est.2017.12.004>.
- [25] T. El Achkar, S. Fourmentin, H. Greige-Gerges, Deep eutectic solvents: an overview on their interactions with water and biochemical compounds, *J. Mol. Liq.* 288 (2019) 111028, <https://doi.org/10.1016/j.molliq.2019.111028>.
- [26] A. Manuscript, Green Chemistry, Extr. Desulfurization Process Fuels with Ammonium-Based Deep Eutectic Solvents, vol. 15, 2013, pp. 2793–2799, <https://doi.org/10.1039/b000000x>.
- [27] B. Gurkan, H. Squire, E. Pentzer, Metal-free deep eutectic solvents: preparation, physical properties, and significance, *J. Phys. Chem. Lett.* 10 (2019) 7956–7964, <https://doi.org/10.1021/acs.jpcclett.9b01980>.
- [28] N. Rodriguez Rodriguez, A. Van Den Bruinhorst, L.J.B.M. Kollau, M.C. Kroon, K. Binnemans, Degradation of deep-eutectic solvents based on choline chloride and carboxylic acids, *ACS Sustain. Chem. Eng.* 7 (2019) 11521–11528, <https://doi.org/10.1021/acssuschemeng.9b01378>.
- [29] N. Ricky Saputra, Rashmi Walvekar, Mohammad Khalid, M. Mubarak, Synthesis and thermophysical properties of ethylammonium chloride-glycerol-ZnCl₂ ternary deep eutectic solvent, *J. Mol. Liq.* (2020) 113232, <https://doi.org/10.1016/j.molliq.2020.113232>.
- [30] W. Yang, X. Du, J. Zhao, W. Yang, X. Du, J. Zhao, Z. Chen, J. Li, J. Xie, Y. Zhang, Article hydrated eutectic electrolytes with ligand- oriented solvation shells for long-cycling zinc-organic batteries hydrated eutectic electrolytes with ligand-oriented solvation shells for long-cycling zinc-organic batteries, *Joule* (2020) 1–18, <https://doi.org/10.1016/j.joule.2020.05.018>.
- [31] H. Ogawa, H. Mori, Lithium salt/amide-based deep eutectic electrolytes for lithium-ion batteries: electrochemical, thermal and computational study, *Phys. Chem. Chem. Phys.* 22 (2020) 8853–8863, <https://doi.org/10.1039/d0cp01255f>.
- [32] G. Li, H. Yang, D. Zuo, J. Xu, H. Zhang, Deep eutectic solvent-based supramolecular gel polymer electrolytes for high-performance electrochemical double layer capacitors, *Int. J. Hydrogen Energy* 46 (2021) 13044–13049, <https://doi.org/10.1016/j.ijhydene.2021.01.158>.
- [33] V. Verma, R.M. Chan, L.J. Yang, S. Kumar, S. Sattayaporn, R. Chua, Y. Cai, P. Kidkhunthod, W. Manalastas, M. Srinivasan, Chelating ligands as electrolyte solvent for rechargeable zinc-ion batteries, *Chem. Mater.* 33 (2021) 1330–1340, <https://doi.org/10.1021/acs.chemmater.0c04358>.
- [34] S. Azmi, M.F. Koudahi, E. Frackowiak, Reline deep eutectic solvent as a green electrolyte for electrochemical energy storage applications, *Energy Environ. Sci.* 15 (2022) 1156–1171, <https://doi.org/10.1039/d1ee02920g>.
- [35] J. Chen, M. Zhu, M. Gan, X. Wang, C. Gu, J. Tu, Rapid electrodeposition and corrosion behavior of Zn coating from a designed deep eutectic solvent, *Metals (Basel)*. 13 (2023), <https://doi.org/10.3390/met13010172>.
- [36] F.A. Getie, D.W. Ayele, N.G. Habtu, T.A. Yemata, F.A. Yihun, M.D. Ambaw, A.K. Worku, Development of zinc nitrate hexahydrate salt (ZNH)/ethylene glycol (EG) binary composite deep eutectic electrolytes, *Int. J. Electrochem. Sci.* 19 (2024) 100616, <https://doi.org/10.1016/j.ijoes.2024.100616>.
- [37] F.A. Getie, D.W. Ayele, N.G. Habtu, T.A. Yemata, F.A. Yihun, Electrochemical and physicochemical properties of zinc(II) nitrate hexahydrate/urea/ethylene glycol ternary composite deep eutectic solvents, *Ionics (Kiel)* (2024), <https://doi.org/10.1007/s11581-024-05672-5>.
- [38] M.I. Martín, I. García-Díaz, M.L. Rodríguez, M.C. Gutiérrez, F. del Monte, F.A. López, Synthesis and properties of hydrophilic and hydrophobic deep eutectic solvents via heating-stirring and ultrasound, *Molecules* 29 (2024) 1–20, <https://doi.org/10.3390/molecules29133089>.
- [39] A. Yadav, S. Pandey, Densities and Viscosities of (Choline Chloride + Urea) Deep Eutectic Solvent and its Aqueous Mixtures in the Temperature Range 293.15 K to 363.15 K, 2014.
- [40] M.C. Gutiérrez, M.L. Ferrer, L. Yuste, F. Rojo, F. del Monte, Bacteria incorporation in deep-eutectic solvents through freeze-drying, *Angew. Chem.* 122 (2010) 2204–2208, <https://doi.org/10.1002/ange.200905212>.
- [41] M.Q. Farooq, N.M. Abbasi, J.L. Anderson, Deep eutectic solvents in separations: methods of preparation, polarity, and applications in extractions and capillary electrochromatography, *J. Chromatogr., A* 1633 (2020) 461613, <https://doi.org/10.1016/j.chroma.2020.461613>.
- [42] P.L. Pisano, M. Espino, M.D.L. Ángeles, M.F. Silva, A.C. Olivieri, PT NU, *Microchem. J.* 143 (2018) 252–258, <https://doi.org/10.1016/j.microc.2018.08.016>.
- [43] A.Y. Dai, J. Van Spronsen, G. Witkamp, Natural deep eutectic solvents as new potential media for green technology, *Anal. Chim. Acta* 766 (2012) 61–68, <https://doi.org/10.1016/j.aca.2012.12.019>.
- [44] A. Paiva, R. Craveiro, I. Aroso, M. Martins, R.L. Reis, A.R.C. Duarte, Natural deep eutectic solvents - solvents for the 21st century, *ACS Sustain. Chem. Eng.* 2 (2014) 1063–1071, <https://doi.org/10.1021/sc500096j>.
- [45] C. Florindo, F.S. Oliveira, L.P.N. Rebelo, A.M. Fernandes, I.M. Marucho, Insights into the synthesis and properties of deep eutectic solvents based on cholinium chloride and carboxylic acids, *ACS Sustain. Chem. Eng.* 2 (2014) 2416–2425, <https://doi.org/10.1021/sc500439w>.
- [46] Y. Cui, C. Li, J. Yin, S. Li, Y. Jia, M. Bao, Design, Synthesis and Properties of Acidic Deep Eutectic Solvents Based on Choline Chloride, Elsevier B.V, 2017, <https://doi.org/10.1016/j.molliq.2017.04.052>.
- [47] D.E. Crawford, C.K.G. Miskimmin, A.B. Albadarin, G. Walker, S.L. James, Organic synthesis by twin screw extrusion (TSE): continuous, scalable and solvent-free, *Green Chem.* 19 (2017) 1507–1518, <https://doi.org/10.1039/c6gc03413f>.
- [48] D.E. Crawford, L.A. Wright, S.L. James, A.P. Abbott, Efficient continuous synthesis of high purity deep eutectic solvents by twin screw extrusion, *Chem. Commun.* 52 (2016) 4215–4218, <https://doi.org/10.1039/c5cc09685e>.
- [49] F.J.V. Gomez, M. Espino, M.A. Fernández, M.F. Silva, A greener approach to prepare natural deep eutectic solvents, *ChemistrySelect* 3 (2018) 6122–6125, <https://doi.org/10.1002/slct.201800713>.
- [50] A.P.R. Santana, J.A. Mora-Vargas, T.G.S. Guimarães, C.D.B. Amaral, A. Oliveira, M.H. Gonzalez, Sustainable synthesis of natural deep eutectic solvents (NADES) by different methods, *J. Mol. Liq.* 293 (2019) 111452, <https://doi.org/10.1016/j.molliq.2019.111452>.
- [51] M. Reynolds, L.M. Duarte, W.K.T. Coltro, M.F. Silva, F.J.V. Gomez, C.D. Garcia, Laser-engraved ammonia sensor integrating a natural deep eutectic solvent, *Microchem. J.* 157 (2020) 105067, <https://doi.org/10.1016/j.microc.2020.105067>.
- [52] X. Wang, Y. Wu, J. Li, A. Wang, G. Li, X. Ren, W. Yin, Ultrasound-assisted deep eutectic solvent extraction of echinacoside and oleuropein from *Syringia pubescens* Turcz, *Ind. Crops Prod.* 151 (2020) 112442, <https://doi.org/10.1016/j.indcrop.2020.112442>.
- [53] A. Tzani, S. Kalafateli, G. Tatsis, M. Bairaktari, I. Kostopoulou, A.R.N. Pontillo, A. Detsi, Natural deep eutectic solvents (NaDESs) as alternative green extraction media for ginger (*Zingiber officinale* Roscoe), *Sustain. Chem.* 2 (2021) 576–599, <https://doi.org/10.3390/suschem2040032>.
- [54] E.L. Smith, A.P. Abbott, K.S. Ryder, Deep eutectic solvents (DESs) and their applications, *Chem. Rev.* 114 (2014) 11060–11082, <https://doi.org/10.1021/cr300162p>.
- [55] Q. Zhang, K. De Oliveira Vigier, S. Royer, F. Jérôme, Deep eutectic solvents: syntheses, properties and applications, *Chem. Soc. Rev.* 41 (2012) 7108–7146, <https://doi.org/10.1039/c2cs35178a>.
- [56] A. Umar, M. Munir, M. Murtaza, R. Sultana, M.A. Riaz, G.R. Srinivasan, A. Firdous, M. Saeed, Properties and green applications based review on highly efficient deep eutectic solvents, *Egypt. J. Chem.* 63 (2020) 59–69, <https://doi.org/10.21608/ejchem.2019.12604.1782>.
- [57] A. Yadav, S. Pandey, Densities and viscosities of (choline chloride + urea) deep eutectic solvent and its aqueous mixtures in the temperature range 293.15 K to 363.15 K, *J. Chem. Eng. Data* 59 (2014) 2221–2229, <https://doi.org/10.1021/je5001796>.
- [58] R.K. Ibrahim, M. Hayyan, M.A. AlSaadi, S. Ibrahim, A. Hayyan, M.A. Hashim, Physical properties of ethylene glycol-based deep eutectic solvents, *J. Mol. Liq.* 276 (2019) 794–800, <https://doi.org/10.1016/j.molliq.2018.12.032>.
- [59] A.P. Abbott, J.C. Barron, K.S. Ryder, D. Wilson, Eutectic-based ionic liquids with metal-containing anions and cations, *Chem. Eur. J.* 13 (2007) 6495–6501, <https://doi.org/10.1002/chem.200601738>.
- [60] I. Wazeer, M. Hayyan, M.K. Hadj-Kali, Deep eutectic solvents: designer fluids for chemical processes, *J. Chem. Technol. Biotechnol.* 93 (2018) 945–958, <https://doi.org/10.1002/jctb.5491>.
- [61] H. Qin, X. Hu, J. Wang, H. Cheng, L. Chen, Z. Qi, Overview of acidic deep eutectic solvents on synthesis, properties and applications, *Green Energy Environ.* 5 (2020) 8–21, <https://doi.org/10.1016/j.gee.2019.03.002>.
- [62] G. García, S. Aparicio, R. Ullah, M. Atilhan, Deep eutectic solvents: physicochemical properties and gas separation applications, *Energy Fuel.* 29 (2015) 2616–2644, <https://doi.org/10.1021/ef5028873>.

- [63] M. Hayyan, T. Aissaoui, M.A. Hashim, M.A.H. AlSaadi, A. Hayyan, Triethylene glycol based deep eutectic solvents and their physical properties, *J. Taiwan Inst. Chem. Eng.* 50 (2015) 24–30, <https://doi.org/10.1016/j.jtice.2015.03.001>.
- [64] Z. Yuan, H. Liu, W.F. Yong, Q. She, J. Esteban, Status and advances of deep eutectic solvents for metal separation and recovery, *Green Chem.* 24 (2022) 1895–1929, <https://doi.org/10.1039/d1gc03851f>.
- [65] F.S. Ghareh Bagh, K. Shahbaz, F.S. Mjalli, M.A. Hashim, I.M. Alnashef, Zinc (II) chloride-based deep eutectic solvents for application as electrolytes: preparation and characterization, *J. Mol. Liq.* 204 (2015) 76–83, <https://doi.org/10.1016/j.molliq.2015.01.025>.
- [66] A.P. Abbott, G. Capper, S. Gray, Design of improved deep eutectic solvents using hole theory, *ChemPhysChem* 7 (2006) 803–806, <https://doi.org/10.1002/cphc.200500489>.
- [67] M.A. Kareem, F.S. Mjalli, M.A. Hashim, I.M. Alnashef, Phosphonium-based ionic liquids analogues and their physical properties, *J. Chem. Eng. Data* 55 (2010) 4632–4637, <https://doi.org/10.1021/jc100104v>.
- [68] M.K. Alomar, M. Hayyan, M.A. Alsaadi, S. Akib, A. Hayyan, M.A. Hashim, Glycerol-based deep eutectic solvents: physical properties, *J. Mol. Liq.* 215 (2016) 98–103, <https://doi.org/10.1016/j.molliq.2015.11.032>.
- [69] I. Delcheva, D.A. Beattie, J. Ralston, M. Krasowska, Dynamic wetting of imidazolium-based ionic liquids on gold and glass, *Phys. Chem. Chem. Phys.* 20 (2018) 2084–2093, <https://doi.org/10.1039/c7cp06404g>.
- [70] J. Klomfar, M. Součková, J. Pátek, Surface tension and density for members of four ionic liquid homologous series containing a pyridinium based-cation and the bis(trifluoromethylsulfonyl)imide anion, *Fluid Phase Equil.* 431 (2017) 24–33, <https://doi.org/10.1016/j.fluid.2016.10.004>.
- [71] T.M. Koller, M.H. Rausch, K. Pohako-Esko, P. Wasserscheid, A.P. Fröba, Surface tension of tricyanomethanide- and tetracyanoborate-based imidazolium ionic liquids by using the pendant drop method, *J. Chem. Eng. Data* 60 (2015) 2665–2673, <https://doi.org/10.1021/acs.jced.5b00303>.
- [72] H.Z. Su, J.M. Yin, Q.S. Liu, C.P. Li, Properties of four deep eutectic solvents: density, electrical conductivity, dynamic viscosity and refractive index, *Wuli Huaxue Xuebao/Acta Phys. - Chim. Sin.* 31 (2015) 1468–1473, <https://doi.org/10.3866/PKU.WHXB201506111>.
- [73] P.B. Sánchez, B. González, J. Salgado, J. José Parajó, Á. Domínguez, Physical properties of seven deep eutectic solvents based on L-proline or betaine, *J. Chem. Thermodyn.* 131 (2019) 517–523, <https://doi.org/10.1016/j.jct.2018.12.017>.
- [74] S. Ravula, N.E. Larm, M.A. Mottaleb, M.P. Heitz, G.A. Baker, Vapor pressure mapping of ionic liquids and low-volatility fluids using graded isothermal thermogravimetric analysis, *ChemEngineering* 3 (2019) 1–12, <https://doi.org/10.3390/chemengineering3020042>.
- [75] A.A.M. Elgharabawy, M. Hayyan, A. Hayyan, W.J. Basirun, H.M. Salleh, M.E.S. Mirghani, A grand avenue to integrate deep eutectic solvents into biomass processing, *Biomass Bioenergy* 137 (2020) 105550, <https://doi.org/10.1016/j.biombioe.2020.105550>.
- [76] A. Hayyan, F.S. Mjalli, I.M. Alnashef, Y.M. Al-Wahaibi, T. Al-Wahaibi, M.A. Hashim, Glucose-based deep eutectic solvents: physical properties, *J. Mol. Liq.* 178 (2013) 137–141, <https://doi.org/10.1016/j.molliq.2012.11.025>.
- [77] A. Skulcova, A. Russ, M. Jablonsky, J. Sima, The pH behavior of seventeen deep eutectic solvents, *Bioresources* 13 (2019) 5042–5051, <https://doi.org/10.15376/biores.13.3.5042-5051>.
- [78] N. Delgado-Mellado, M. Larriba, P. Navarro, V. Rigual, M. Ayuso, J. García, F. Rodríguez, Thermal stability of choline chloride deep eutectic solvents by TGA/FTIR-ATR analysis, *J. Mol. Liq.* 260 (2018) 37–43, <https://doi.org/10.1016/j.molliq.2018.03.076>.
- [79] Bhawna, A. Pandey, S. Pandey, Superbase-added choline chloride-based deep eutectic solvents for CO₂ capture and sequestration, *ChemistrySelect* 2 (2017) 11422–11430, <https://doi.org/10.1002/slct.201702259>.
- [80] A. Basaiahgari, S. Panda, R.L. Gardas, Effect of ethylene, diethylene, and triethylene glycols and glycerol on the physicochemical properties and phase behavior of benzyltrimethyl and benzyltributylammonium chloride based deep eutectic solvents at 283.15–343.15 K, *J. Chem. Eng. Data* 63 (2018) 2613–2627, <https://doi.org/10.1021/acs.jced.8b00213>.
- [81] H.G. Morrison, C.C. Sun, S. Neervannan, Characterization of thermal behavior of deep eutectic solvents and their potential as drug solubilization vehicles, *Int. J. Pharm.* 378 (2009) 136–139, <https://doi.org/10.1016/j.ijpharm.2009.05.039>.
- [82] I. De Las Heras, J. Dufour, B. Coto, A novel method to obtain solid–liquid equilibrium and eutectic points for hydrocarbon mixtures by using differential scanning calorimetry and numerical integration, *Fuel* 297 (2021) 120788, <https://doi.org/10.1016/j.fuel.2021.120788>.
- [83] M. Francisco, A. Van Den Bruinhorst, M.C. Kroon, New natural and renewable low transition temperature mixtures (LTTMs): screening as solvents for lignocellulosic biomass processing, *Green Chem.* 14 (2012) 2153–2157, <https://doi.org/10.1039/c2gc35660k>.
- [84] I. Dello, C. Lafuente, J. Muñoz-Embida, M. Artal, NMR study of choline chloride-based deep eutectic solvents, *J. Mol. Liq.* 290 (2019) 111236, <https://doi.org/10.1016/j.molliq.2019.111236>.
- [85] D.J.G.P. Van Osch, C.H.J.T. Dietz, J. Van Spronsen, M.C. Kroon, F. Gallucci, M. Van Sint Annaland, R. Tuinier, A search for natural hydrophobic deep eutectic solvents based on natural components, *ACS Sustain. Chem. Eng.* 7 (2019) 2933–2942, <https://doi.org/10.1021/acssuschemeng.8b03520>.
- [86] N. Siraj, B. El-Zahab, S. Hamdan, T.E. Karam, L.H. Haber, M. Li, S.O. Fakayode, S. Das, B. Valle, R.M. Strongin, G. Patonay, H.O. Sintim, G.A. Baker, A. Powe, M. Lowry, J.O. Karolin, C.D. Geddes, I.M. Warner, Fluorescence, phosphorescence, and chemiluminescence, *Anal. Chem.* 88 (2016) 170–202, <https://doi.org/10.1021/acs.analchem.5b04109>.
- [87] A. Pandey, R. Rai, M. Pal, S. Pandey, How polar are choline chloride-based deep eutectic solvents? *Phys. Chem. Chem. Phys.* 16 (2014) 1559–1568, <https://doi.org/10.1039/c3cp53456a>.
- [88] A. Kadyan, K. Behera, S. Pandey, Hybrid green nonaqueous media: tetraethylene glycol modifies the properties of a (choline chloride + urea) deep eutectic solvent, *RSC Adv.* 6 (2016) 29920–29930, <https://doi.org/10.1039/C6RA03726G>.
- [89] A. Pandey, S. Pandey, Solvatochromic probe behavior within choline chloride-based deep eutectic solvents: effect of temperature and water, *J. Phys. Chem. B* 118 (2014) 14652–14661, <https://doi.org/10.1021/jp510420h>.
- [90] D. Dhingra, B. Bhawna, A. Pandey, S. Pandey, Pyrene Fluorescence to Probe a Lithium Chloride-Added (Choline Chloride + Urea) Deep Eutectic Solvent, 2019, <https://doi.org/10.1021/acs.jpcc.9b01193>.
- [91] A. Pandey, Bhawna, D. Dhingra, S. Pandey, Hydrogen bond donor/acceptor cosolvent-modified choline chloride-based deep eutectic solvents. <https://doi.org/10.1021/acs.jpcc.7b01724>, 2017.
- [92] X. Lu, E.J. Hansen, G. He, J. Liu, Eutectic electrolytes chemistry for rechargeable Zn batteries, *Small* 18 (2022) 1–20, <https://doi.org/10.1002/smll.202200550>.
- [93] C. D'Agostino, R.C. Harris, A.P. Abbott, L.F. Gladden, M.D. Mantle, Molecular motion and ion diffusion in choline chloride based deep eutectic solvents studied by 1H pulsed field gradient NMR spectroscopy, *Phys. Chem. Chem. Phys.* 13 (2011) 21383–21391, <https://doi.org/10.1039/c1cp22554e>.
- [94] S.N.S. Nasir, N. Sidek, M.F.Z. Kadir, N.S.A. Manan, Electrochemical behavior of NH₄VO₃ in glycine DES studied by cyclic voltammetry method, *Ionics (Kiel)* 25 (2019) 4981–4990, <https://doi.org/10.1007/s11581-019-03054-w>.
- [95] A. Renjith, V. Lakshminarayanan, Electron-transfer studies of model redox-active species (cationic, anionic, and neutral) in deep eutectic solvents, *J. Phys. Chem. C* 122 (2018) 25411–25421, <https://doi.org/10.1021/acs.jpcc.8b07749>.
- [96] O.A. von Lilienfeld, Quantum machine learning in chemical compound space, *Angew. Chem. Int. Ed.* 57 (2018) 4164–4169, <https://doi.org/10.1002/anie.201709686>.
- [97] S. Kaur, M. Kumari, H.K. Kashyap, Microstructure of deep eutectic solvents: current understanding and challenges, *J. Phys. Chem. B* 124 (2020) 10601–10616, <https://doi.org/10.1021/acs.jpcc.0c07934>.
- [98] C.G. Hanke, S.L. Price, R.M. Lynden-Bell, Intermolecular potentials for simulations of liquid imidazolium salts, *Mol. Phys.* 99 (2001) 801–809, <https://doi.org/10.1080/00268970010018981>.
- [99] J.M. Rimsza, L.R. Corrales, Adsorption complexes of copper and copper oxide in the deep eutectic solvent 2:1 urea-choline chloride, *Comput. Theor. Chem.* 987 (2012) 57–61, <https://doi.org/10.1016/j.comptc.2011.11.003>.
- [100] H. Sun, Y. Li, X. Wu, G. Li, Theoretical study on the structures and properties of mixtures of urea and choline chloride, *J. Mol. Model.* 19 (2013) 2433–2441, <https://doi.org/10.1007/s00894-013-1791-2>.

- [101] C.R. Ashworth, R.P. Matthews, T. Welton, P.A. Hunt, Doubly ionic hydrogen bond interactions within the choline chloride-urea deep eutectic solvent, *Phys. Chem. Chem. Phys.* 18 (2016) 18145–18160, <https://doi.org/10.1039/c6cp02815b>.
- [102] Y. Shen, X. He, F.R. Hung, Structural and dynamical properties of a deep eutectic solvent confined inside a slit pore, *J. Phys. Chem. C* 119 (2015) 24489–24500, <https://doi.org/10.1021/acs.jpcc.5b08172>.
- [103] L. Mixtures, The role of charge transfer in the formation of type, *Molecules* 24 (2019) 3687.
- [104] P.A. Hunt, C.R. Ashworth, R.P. Matthews, Hydrogen bonding in ionic liquids, *Chem. Soc. Rev.* 44 (2015) 1257–1288, <https://doi.org/10.1039/c4cs00278d>.
- [105] D.V. Wagle, G.A. Baker, E. Mamontov, Differential microscopic mobility of components within a deep eutectic solvent, *J. Phys. Chem. Lett.* 6 (2015) 2924–2928, <https://doi.org/10.1021/acs.jpcclett.5b01192>.
- [106] M. Rück, B. Garlyyev, F. Mayr, A.S. Bandarenka, A. Gagliardi, Oxygen reduction activities of strained platinum core-shell electrocatalysts predicted by machine learning, *J. Phys. Chem. Lett.* 11 (2020) 1773–1780, <https://doi.org/10.1021/acs.jpcclett.0c00214>.
- [107] Y. Xie, C. Zhang, X. Hu, C. Zhang, S.P. Kelley, J.L. Atwood, J. Lin, Machine learning assisted synthesis of metal-organic nanocapsules, *J. Am. Chem. Soc.* 142 (2020) 1475–1481, <https://doi.org/10.1021/jacs.9b11569>.
- [108] A. Fabrizio, A. Grisafi, B. Meyer, M. Ceriotti, C. Corminboeuf, Electron density learning of non-covalent systems, *Chem. Sci.* 10 (2019) 9424–9432, <https://doi.org/10.1039/c9sc02696g>.
- [109] T. Morawietz, A.S. Urbina, P.K. Wise, X. Wu, W. Lu, D. Ben-Amotz, T.E. Markland, Hiding in the crowd: spectral signatures of overcoordinated hydrogen-bond environments, *J. Phys. Chem. Lett.* 10 (2019) 6067–6073, <https://doi.org/10.1021/acs.jpcclett.9b01781>.
- [110] Y. Zhang, Z. Chen, H. Qiu, W. Yang, Z. Zhao, J. Zhao, G. Cui, Pursuit of reversible Zn electrochemistry: a time-honored challenge towards low-cost and green energy storage, *NPG Asia Mater.* 12 (2020) 1–24, <https://doi.org/10.1038/s41427-019-0167-1>.
- [111] G.M. Thorat, V.C. Ho, J. Mun, Zn-based deep eutectic solvent as the stabilizing electrolyte for Zn metal anode in rechargeable aqueous batteries, *Front. Chem.* 9 (2022) 2–9, <https://doi.org/10.3389/fchem.2021.825807>.
- [112] W. Yang, X. Du, J. Zhao, Z. Chen, J. Li, J. Xie, Y. Zhang, Z. Cui, Q. Kong, Z. Zhao, C. Wang, Q. Zhang, G. Cui, Hydrated eutectic electrolytes with ligand-oriented solvation shells for long-cycling zinc-organic batteries, *Joule* 4 (2020) 1557–1574, <https://doi.org/10.1016/j.joule.2020.05.018>.
- [113] V. Verma, R.M. Chan, L. Jia Yang, S. Kumar, S. Sattayaporn, R. Chua, Y. Cai, P. Kidkhunthod, W. Manalastas, M. Srinivasan, Chelating ligands as electrolyte solvent for rechargeable zinc-ion batteries, *Chem. Mater.* 33 (2021) 1330–1340, <https://doi.org/10.1021/acs.chemmater.0c04358>.
- [114] L. Wang, Y. Zhang, H. Hu, H.Y. Shi, Y. Song, D. Guo, X.X. Liu, X. Sun, A Zn(ClO₄)₂ electrolyte enabling long-life zinc metal electrodes for rechargeable aqueous zinc batteries, *ACS Appl. Mater. Interfaces* (2019), <https://doi.org/10.1021/acsami.9b10905>.
- [115] R. Chen, C. Zhang, J. Li, Z. Du, F. Guo, W. Zhang, Y. Dai, W. Zong, X. Gao, J. Zhu, Y. Zhao, X. Wang, G. He, A hydrated deep eutectic electrolyte with finely-tuned solvation chemistry for high-performance zinc-ion batteries, *Energy Environ. Sci.* 16 (2023) 2540–2549, <https://doi.org/10.1039/d3ee00462g>.
- [116] T. Jurić, D. Uka, B.B. Holló, B. Jović, B. Kordić, B.M. Popović, Comprehensive physicochemical evaluation of choline chloride-based natural deep eutectic solvents, *J. Mol. Liq.* 343 (2021), <https://doi.org/10.1016/j.molliq.2021.116968>.
- [117] M. Hayyan, A. Hayyan, A.D.M. Hafizi, W.J. Basirun, A.T.H. Yeow, M.Z.M. Salleh, H. Saputra, J. Saleh, K.H. Alkandari, M.A. Hashim, M.A. Alsaadi, Phosphonium-based deep eutectic solvents: physicochemical properties and application in Zn-air battery, *Chem. Eng. Process. - Process Intensif.* 185 (2023) 109310, <https://doi.org/10.1016/j.cep.2023.109310>.